Inhibitors

Exploiting Atropisomerism to Increase the Target Selectivity of Kinase Inhibitors

Davis E. Smith, Isaac Marquez, Melissa E. Lokensgard, Arnold L. Rheingold, David A. Hecht, and Jeffrey L. Gustafson

Abstract: Many biologically active molecules exist as rapidly interconverting atropisomeric mixtures. Whereas one atropisomer inhibits the desired target, the other can lead to off-target effects. Herein, we study atropisomerism as a possibility to improve the selectivities of kinase inhibitors through the synthesis of conformationally stable pyrrolopyrimidines. Each atropisomer was isolated by HPLC on a chiral stationary phase and subjected to inhibitor profiling across a panel of 18 tyrosine kinases. Notably different selectivity patterns between atropisomers were observed, as well as improved selectivity compared to a rapidly interconverting parent molecule. Computational docking studies then provided insights into the structure-based origins of these effects. This study is one of the first examples of the intentional preorganization of a promiscuous scaffold along an atropisomeric axis to increase target selectivity, and provides fundamental insights that may be applied to other atropisomeric target scaffolds.

The human genome contains over 500 protein kinases, which affect intracellular signal transduction pathways through protein phosphorylation.[1] Aberrant kinase activity has been implicated in numerous diseases,[2] leading to an intense drug discovery effort to develop efficacious anti-kinase therapeutics that has resulted in over 20 FDA-approved targeted kinase inhibitors mainly for the treatment of cancers, including chronic myeloid leukemia and non-small-cell lung cancer.[3] Although these efforts have revolutionized cancer therapy, a large degree of active-site conservation throughout the kinase family causes most kinase inhibitors to possess promiscuous inhibition activities towards many kinases. While often needed for a complete response,[4,5] this poly-pharmacology can also lead to side effects that negatively influence the quality of life,[6,7] largely preventing kinase inhibitors from becoming therapeutics for chronic non-lethal diseases, such as rheumatoid arthritis, where selectivity becomes a much larger requirement.[8]

Kinase inhibitors are also common chemical probes to elucidate the role of a kinase or signaling pathways in cellular processes or disease. These fundamental studies are frequently confounded by off-target kinase inhibition affecting unintended signaling pathways.[9–12] In recent years, chemists and biologists have begun to gain an understanding of factors that can contribute to increasing the selectivity of a small molecule towards a specific kinase using "selectivity filters" that take advantage of unusual features in a kinase active site to obtain highly selective kinase inhibitors.[13–16] A general selectivity filter has remained elusive as by design they rely on rare occurrences in an active site. In this fundamental work, we study atropisomer conformation as a selectivity filter in kinase inhibition.

Atropisomerism is a form of chirality that arises from hindered rotation around an axis that renders the rotational isomers enantiomers. Many biologically active small molecules possess little hindrance to rotation and exist as rapidly interconverting mixtures of atropisomers,[17] yet bind to their respective biological targets in an atropisomer-specific manner. This dynamic nature of atropisomerism can cause serious complications in drug development, as atropisomers can display drastically different pharmacological profiles.[18–21] This often results in confounding effects caused by the non-target-relevant atropisomer, particularly when a compound possesses an intermediate stability, and can racemize over the length of the experiment.[22,23]

In recent reports, researchers have synthesized atropisomerically stable analogues of a lead molecule and observed strikingly differential target affinities between the separated atropisomers,[17,24] including a seminal report with a p38 MAP kinase inhibitor.[25] Recent literature also suggests that atropisomerically pure analogues can posses an improved toxicological profile as the non-target-binding atropisomer is precluded.[26] For example, Yoshida[27] and co-workers have recently synthesized atropisomeric lamellarin analogues, and found that each atropisomer possesses a notably different kinase inhibition profile with one atropisomer displaying improved selectivity compared to the parent molecule.

As several kinase inhibitors are rapidly interconverting atropisomers (Figure 1 A), we set out to evaluate atropisomerism as a strategy to improve upon the selectivity of promiscuous kinase inhibitors. For these initial studies, we chose pyrrolopyrimidine-based kinase inhibitors (PPYs) as they represent a common and promiscuous kinase inhibitor scaffold that often possesses at least one atropisomeric axis (Figure 1 B).[28,29] Furthermore, the identification of PPY

[*] D. E. Smith, I. Marquez, M. E. Lokensgard, Prof. J. L. Gustafson
Department of Chemistry and Biochemistry
San Diego State University
5500 Campanile Drive, San Diego, CA 92182-1030 (USA)
E-mail: JGustafson@mail.sdsu.edu

Prof. A. L. Rheingold
Department of Chemistry and Biochemistry
University of California at San Diego
La Jolla, CA 92093-0385 (USA)

Prof. D. A. Hecht
School of Mathematics, Science & Engineering
Southwestern College
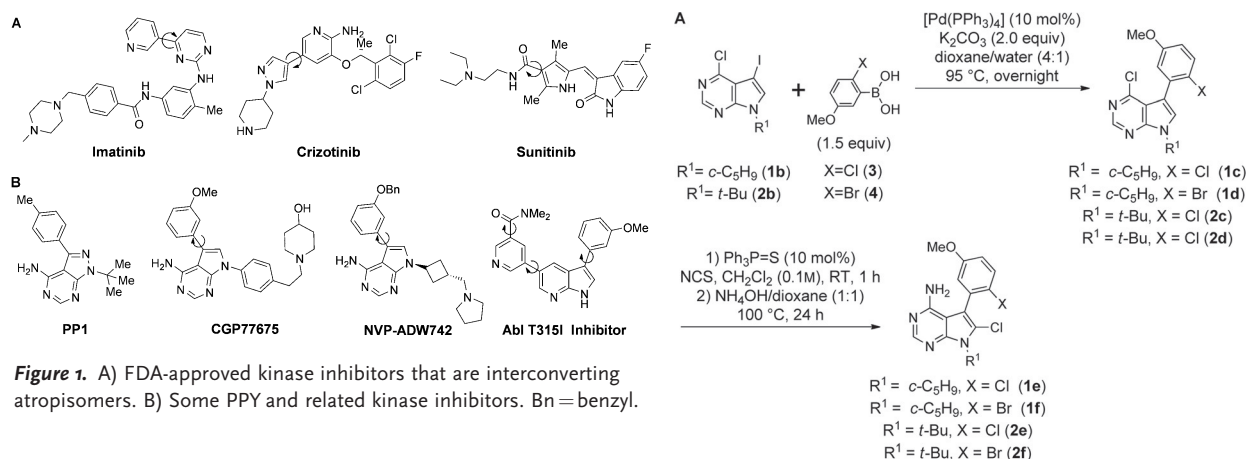900 Otay Lakes Rd, Chula Vista, CA 91910 (USA)

Figure 1. A) FDA-approved kinase inhibitors that are interconverting atropisomers. B) Some PPY and related kinase inhibitors. Bn = benzyl.

Figure 2. A) Synthesis of atropisomerically stable PPY kinase inhibitors. B) Traces of the HPLC analysis of **2e** on a chiral stationary phase (Daicel IA) before and after atropisomer separation. C) Circular dichroism spectra of the separated atropisomers of **2e**. D) X-ray crystal structure of the first eluting atropisomer of **1f** (R configuration).[39] E) Experimentally measured barriers to rotation and extrapolated $t_{1/2}$ values to racemization at 37 °C.

analogues with improved kinase selectivities may provide intriguing starting points for drug discovery and towards valuable chemical probes for the investigation of kinase signaling pathways. Fundamentally, PPYs represent an enticing but challenging platform for this work, as although crystallographic analysis (e.g., PDB No. 1YOL) suggests that they indeed bind kinases in an atropisomer-specific manner, PPYs rely primarily on conserved interactions between the kinase active site and the "adenine-like" heterocycle for potency.

First, we developed a simple synthesis of atropisomerically rigidified PPY analogues starting from readily available N-alkylated pyrrolopyrimidines (Figure 2A). The choice of N substitution was based on previous work on PPYs[30] and related (e.g., PP1)[28] kinase inhibitors. Our recently disclosed phosphine sulfide catalyzed halogenation[31] proved crucial throughout this synthesis as it facilitated iodination of the PPY core (to give **1b** and **2b**), boronic acid halogenation (to give **3** and **4**), and the key late-stage chlorination of the PPY core to rigidify the axis in the penultimate step. Nucleophilic aromatic substitution of the chlorine substituent in the 6-position with ammonia led to the racemic PPY analogues **1e**, **1f**, **2e**, and **2f**.

The chlorine substituent proved to be sufficiently large to render the compound stereochemically stable at room temperature with respect to rotation around the PPY–"gate keeper aryl" axis, and each atropisomer was obtained using semi-preparative HPLC on a chiral stationary phase (Figure 2B). Circular dichroism confirmed that the isolated compounds were indeed enantiomeric atropisomers, and X-ray crystallography revealed that the first eluting atropisomer of **1f** was of the R configuration. As the series are structurally similar and were separated using comparable HPLC conditions, we assigned the conformations of **1e**, **2e**, and **2f** by analogy.

We then experimentally measured the barrier to rotation for each series by HPLC,[32] observing stereochemical stabilities ranging from 8 days to 8 years at physiological temperature. Interestingly, we found that the size of the N substituent (R^1) distal to the axis had a clear effect on the barrier to rotation, with tert-butyl substitution increasing the barrier to rotation by 1.2–1.5 kcal mol^{-1} over cyclopentyl substitution, resulting in a change in stereochemical stability at 37 °C from 18 days for **1e** to 157 days for **2e**. This trend is a manifestation
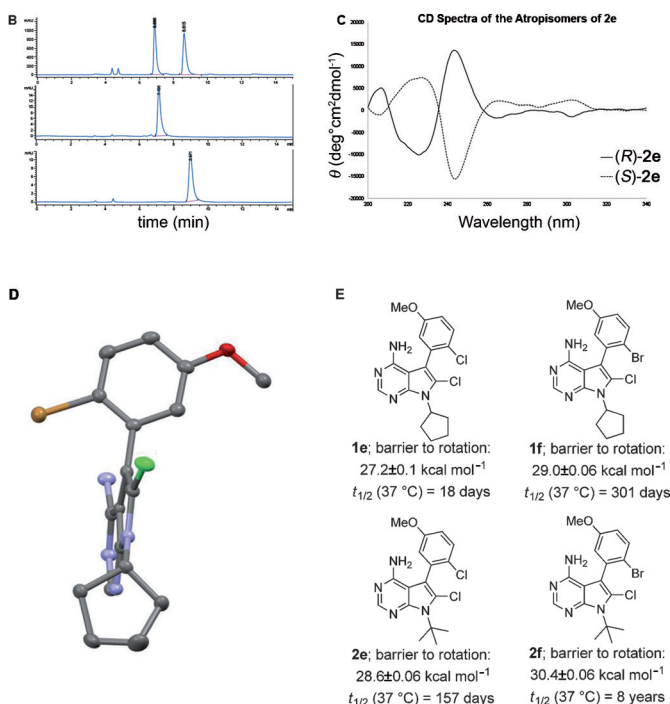
of "the buttress effect"[33] and may represent a strategy to increase stereochemical stabilities when needed.

Based on the observed stereochemical stabilities, we chose **1f**, **2e**, and **2f** for further study and obtained inhibition data against a Src kinase from Life Technologies (Z′-LYTE kinase assay, Figure 3A). Whereas the atropisomeric analogues were roughly 7–14 times less potent than the non-rigidified parent molecule **5**, the atropisomers displayed strikingly differential potencies. For example, whereas the second eluting S atropisomer of **1f** possessed an IC$_{50}$ value of 1300 nM, the first eluting R atropisomer displayed signifi-
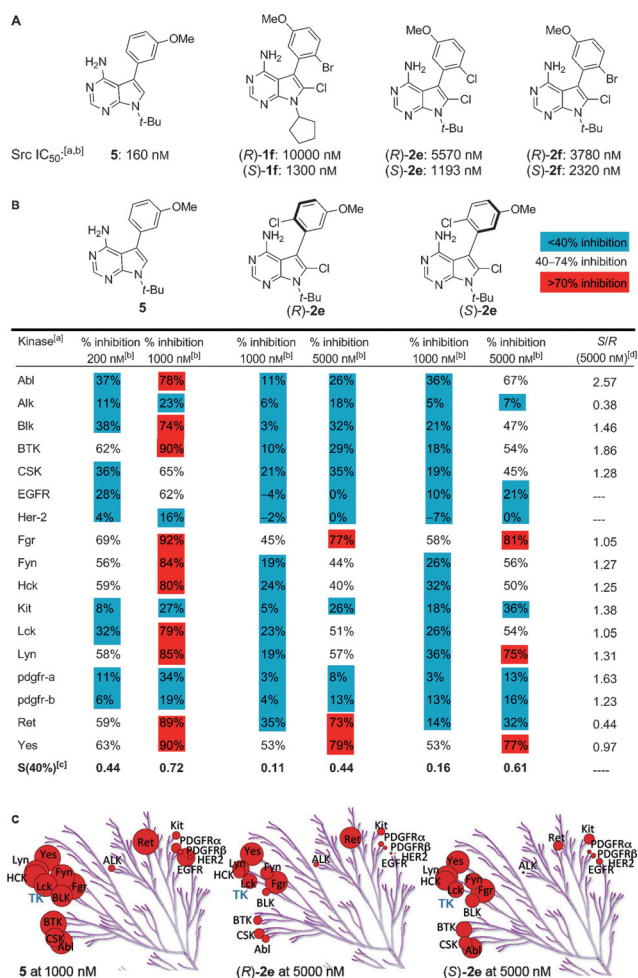
Figure 3. A) Differential Src kinase inhibitory activities between atropisomers. B) Inhibition with **2e** atropisomers and the parent compound across a panel of tyrosine kinases at two different concentrations. C) The tyrosine kinase branch of the kinome annotated with red circles, scaled to percent inhibition. Illustrations reproduced courtesy of Cell Signaling Technology, Inc. (www.cellsignal.com). An error analysis is provided in Figures S1–S6. [a] Data obtained at Life Technologies using the Z'-LYTE kinase inhibition platform. [b] The data is the average of two runs. [c] Number of kinases inhibited by greater than 40% divided by the number of kinases tested (including Src). [d] % inhibition (S)-**2e**/% inhibition (R)-**2e**.

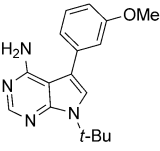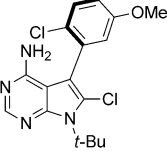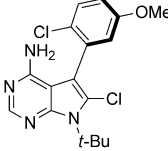| Kinase[a]	% inhibition 200 nM[b]	% inhibition 1000 nM[b]	% inhibition 1000 nM	% inhibition 5000 nM[b]	% inhibition 1000 nM	% inhibition 5000 nM	S/R (5000 nM)[d]
Abl	37%	78%	11%	26%	36%	67%	2.57
Alk	11%	23%	6%	18%	5%	7%	0.38
Blk	38%	74%	3%	32%	21%	47%	1.46
BTK	62%	90%	10%	29%	18%	54%	1.86
CSK	36%	65%	21%	35%	19%	45%	1.28
EGFR	28%	62%	-4%	0%	10%	21%	---
Her-2	4%	16%	-2%	0%	-7%	0%	---
Fgr	69%	92%	45%	77%	58%	81%	1.05
Fyn	56%	84%	19%	44%	26%	56%	1.27
Hck	59%	80%	24%	40%	32%	50%	1.25
Kit	8%	27%	5%	26%	18%	36%	1.38
Lck	32%	79%	23%	51%	26%	54%	1.05
Lyn	58%	85%	19%	57%	36%	75%	1.31
pdgfr-a	11%	34%	3%	8%	3%	13%	1.63
pdgfr-b	6%	19%	4%	13%	13%	16%	1.23
Ret	59%	89%	35%	73%	14%	32%	0.44
Yes	63%	90%	53%	79%	53%	77%	0.97
S(40%)[c]	0.44	0.72	0.11	0.44	0.16	0.61	----

The majority of kinases in the panel preferred the *S* atropisomer to varying degrees; however, comparing the kinase inhibition profiles of the atropisomers of each compound revealed some fascinating differential selectivities. For example, the *R* atropisomer of **2e** was less active towards Src than the *S* atropisomer, yet it inhibited Ret kinase, a validated drug target for numerous cancers, including medullary thyroid cancer,[34–36] to a significantly greater extent than the *S* atropisomer (73% vs. 32% at 5000 nM; Figure 3B). Conversely, the *S* atropisomer inhibited Abl to a significantly greater degree than the *R* atropisomer (67% vs. 26% at 5000 nM). We also performed the profiling experiment with the more potent parent molecule **5**, albeit at lower concentrations to account for its increased potency (200 nM and 1000 nM), finding that **5** possessed near pan activity for the tyrosine kinase panel tested, including significant activity towards Src, Ret, and Abl.

To analyze the selectivity of each analogue across the panel, we turned to selectivity scores,[12] which are simply the number of kinases inhibited above a certain threshold divided by the number of kinases evaluated. The *R* atropisomer was more selective, inhibiting a lower percentage of kinases tested to an intermediate degree (defined as greater than 40% inhibition). For example, at 1000 nM, (*R*)-**2e** yielded an S(40%) value of 0.11 whereas (*S*)-**2e** gave an S(40%) value of 0.16. The parent molecule **5** was less selective at a lower concentration of 200 nM giving an S(40%) value of 0.44 (see Figure 3B). The differences in selectivity between (*R*)-**2e** and (*S*)-**2e** at 5000 nM (4.5 times the IC$_{50}$ of (*S*)-**2e** towards Src) and for **5** at 1000 nM (6.25 times the IC$_{50}$ of **5** towards Src) can be viewed graphically (Figure 3C) across tyrosine kinases.[1] Importantly, similar trends were also observed across each of the atropisomeric series tested (Supporting Information, Figure S1–S6).

We then obtained IC$_{50}$ data for **5** and the **2e** series towards a subset of kinases that displayed differential atropisomeric activities (Src, EGFR, Ret, Abl, YES; Table 1). This data validated the profiling results, and also helped quantitate the differential selectivity between atropisomers. The parent molecule **5** displayed little selectivity towards the kinases tested, with relative selectivity factors of 1.4–2.65 favoring Yes (IC$_{50}$ kinase/IC$_{50}$ YES) over Ret, Src, and Abl, and a selectivity factor of 7 between YES and EGFR. As with the profiling data, the atropisomeric analogues possessed enhanced selectivities compared to **5**. For example, (*R*)-**2e** inhibited Ret kinase with an IC$_{50}$ of 1857 nM, but possessed reduced potency towards Abl and Src (10000 nM and 5570 nM), representing a four-fold augmentation of the inherent selectivity of **5** towards these kinases. Conversely, the *S*-configured isomer was less potent towards Ret (7659 nM, a nearly 8 fold increase of the inherent selectivity of **5**), while maintaining activity towards Src and Abl (1193 nM and 1432 nM). In general, this data demonstrates that different members of highly conserved families of enzymes such as kinases can prefer different atropisomeric conformations of the same inhibitor, and that this can be harnessed to modulate inhibitor promiscuity.

Some kinases in these profiling experiments did not display differential selectivities between atropisomers. For

cantly less potency with an IC$_{50}$ value of greater than 10000 nM. The trend of the first eluting atropisomer possessing attenuated Src inhibitory activity compared to the second eluting atropisomer held throughout each series tested, lending further credence to the conformational assignment based on the X-ray crystal structure of **1f**.

To probe the effect of the atropisomeric conformation on kinase selectivity, we subjected **1f**, **2e**, and **2f** to kinase inhibitor profiling across a panel of tyrosine kinases at 1000 nM and 5000 nM (Data for **2e** shown in Figure 3B). Performing profiling experiments at only a few concentrations is a common practice in the field[3,9] as obtaining IC$_{50}$ data from profiling services can become prohibitively expensive across larger panels.

Table 1: IC$_{50}$ values of atropisomeric kinase inhibitors.

Kinase	IC$_{50}$ **5** [nM]	IC$_{50}$ **5** kinase/ IC$_{50}$ **5** Yes	IC$_{50}$ (R)-**2e** [nM]	IC$_{50}$ (R)-**2e** kinase/ IC$_{50}$ (R)-**2e** Yes	IC$_{50}$ (S)-**2e** [nM]	IC$_{50}$ (S)-**2e** kinase/ IC$_{50}$ (S)-**2e** Yes
Src	151 ± 9[b]	1.64	5570 ± 907[b]	6.22	1193 ± 170[b]	1.64
EGFR	641 ± 54[b]	6.96	>10000[c]	>10	>10000[c]	>10
Yes	92 ± 11[b]	1	895 ± 90[b]	1	727 ± 177[b]	1
Ret	128 ± 3[b]	1.4	1857 ± 482[b]	2.07	7659 ± 754[b]	10.53
Abl	244.5 ± 19[c]	2.65	>10000[c]	>10	1432 ± 210[c]	1.96

[a] Data obtained at Life Technologies using the Z′-LYTE kinase inhibition platform. The error corresponds to the standard deviation. [b] IC$_{50}$ values determined in triplicate. [c] IC$_{50}$ values determined in duplicate.

example, EGFR activity was knocked out across both atropisomers whereas other kinases (Fgr, Yes) maintained comparable activity towards each atropisomer, suggesting that the atropisomeric conformation does not significantly influence binding in these examples.

To gain a better understanding of the physical basis of the observed effects, we turned to molecular modeling. We docked **5** into the known structures of Ret, Src, and EGFR bound to ligands that are structurally similar to PPYs. This experiment predicted that Ret and Src would bind **5** in different atropisomeric conformations, which is in agreement with the observed data and structural assignment (Figure S7). Likewise, this experiment predicted that EGFR would bind both atropisomeric conformations with very little difference in the docking scores. Together, these experiments illustrate that the existence of an inherent atropisomer preference can be predicted in silico, representing a method that allows for the rapid assessment of the utility of applying this approach to a particular kinase target.

We also examined each atropisomer of **2e**. For Src, the (S)-**2e** atropisomer is predicted to fit in the binding site (Figure 4A) and benefit from stabilizing interactions with neighboring Asp 406. The binding mode of (S)-**2e** is consistent with that of CGP77675 (PDB No. 1YOL), which forms the same pyrrolopyrimidine hydrogen bonds and has similar dihedral angles between the two aryl ring systems (57.25° vs. 54.56°).[40] The docked poses also suggest that the preference for (S)-**2e** may arise from small steric clashes between the methoxy group of (R)-**2e** with surrounding residues that are not near the inhibitor when (S)-**2e** is used (Figure 4B).

In Ret, the active atropisomer (R)-**2e** has a binding mode similar to that of PP1 (PDB No. 2IVV), forming the same pyrrolopyrimidine hydrogen bonds and having similar dihedral angles between the two aryl ring systems (−122.57° vs. −116.87°; Figure 4D), and is predicted to benefit from stabilizing interactions with Asp 892 as well as π interactions with a neighboring Lys 758 residue that are not present with (S)-**2e** (Figure 4C). Furthermore, (S)-**2e** is predicted to suffer from a steric clash between the chlorine substituent and Asp 892, which causes the docked pose to shift up with regards

to the X-ray configuration, straining the hydrogen bonds between the pyrrolopyrimidine ring and the neighboring Glu 805 and Ala 807 residues. All of these factors suggest physicochemical origins for the observed (R)-**2e** selectivity towards Ret.

A close examination of the bound (S)-**5** and (R)-**5** poses in the EGFR binding pocket does not predict any additional protein–ligand interactions other than the two pyrrolopyrimidine hydrogen bonds similar to the ones formed by ATP (Figure S8). Both atropisomers seem to fit well in the binding site without apparent steric clashes. In contrast, significant steric clashes seem to exist between the (S)-**2e** methoxy group as well as the (R)-**2e** chlorine substituent with the neighboring
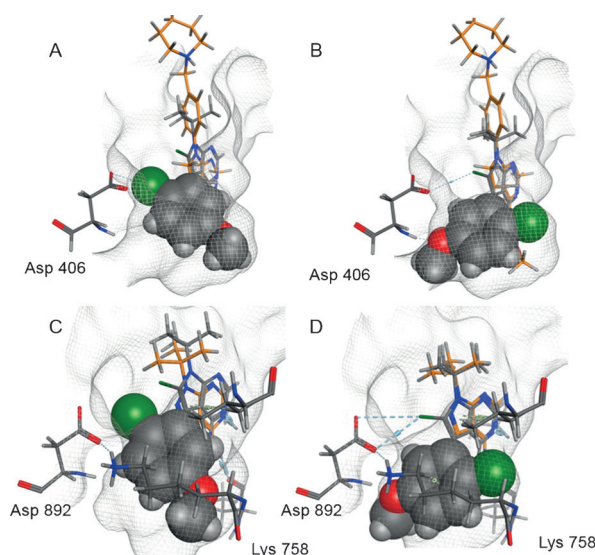

Figure 4. A, B) Structures of (S)-**2e** (A, in gray) and (R)-**2e** (B, in gray) docked to Src overlaid with the electron density of CGP77675 (in gold; PDB No. 1YOL). Interactions with Asp 406 are represented by dashed lines. C, D) Structures of (S)-**2e** (C, in gray) and (R)-**2e** (D, in gray) docked to Ret overlaid with the electron density of PP1 (PDB No. 2IVV). For each structure, the "gate keeper" aryl group of **2e** is shown in space-filling mode. Interactions with the Asp 892 residue and π interactions with Lys 758 are represented by dashed lines.

residues in the ATP binding site. This is consistent with the observed loss of activity. Interestingly, docking studies performed with the inactive form of EGFR[38] (PDB No. 2GS7) resulted in a very clear preference for (*S*)-**2e**. This finding will be explored in future studies.

Taken together, our data suggests that atropisomerism can be leveraged to modulate the selectivity of promiscuous kinase inhibitors. Whereas some of the observed changes in selectivity between **5** and each atropisomer of **2e** may be due to the decreased potency of the analogues, we feel that the differences in the kinase profiles in Table 1 among atropisomers as well as the increased selectivities of (*R*)-**2e** and (*S*)-**2e** at higher concentrations compared to that of **5** suggest that many of the observed differences are due to differential protein recognition towards atropisomers.

To the best of our knowledge, this work represents one of the first examples of the strategic rigidification of a common and promiscuous medicinal-chemistry scaffold around an axis of chirality to improve upon target selectivity. We feel that the presented data illustrates fundamentally that in many cases control of atropisomeric conformation may indeed be leveraged as a general strategy to improve the selectivity profile of kinase inhibitors. Whereas the observed effects on selectivity may be modest compared to those achieved with covalent strategies,[14,37] covalent approaches inherently rely on relatively rare occurrences in the kinase active site limiting their implementation. On the other hand, the ubiquity of atropisomerism in drug discovery should present ample opportunities for it to be applied as a more general approach, often as part of a larger medicinal-chemistry puzzle, to obtain more selective kinase inhibitors.

Acknowledgements

[1] G. Manning, D. B. Whyte, R. Martinez, T. Hunter, S. Sudarsanam, *Science* **2002**, *298*, 1912–1934.
[2] P. Cohen, *Nat. Rev. Drug Discovery* **2002**, *1*, 309–315.
[3] J. Zhang, P. L. Yang, N. S. Gray, *Nat. Rev. Cancer* **2009**, *9*, 28–39.
[4] S. Wong, J. McLaughlin, D. Cheng, C. Zhang, K. M. Shokat, O. N. Witte, *Proc. Natl. Acad. Sci. USA* **2004**, *101*, 17456–17461.
[5] A. Anighoro, J. Bajorath, G. Rastelli, *J. Med. Chem.* **2014**, *57*, 7874–7887.
[6] M. Cornelison, E. J. Jabbour, M. A. Welch, *J. Supportive Oncol.* **2012**, *10*, 14–23.
[7] H. R. Mellor, A. R. Bell, J.-P. Valentin, R. R. A. Roberts, *Toxicol. Sci.* **2011**, *120*, 14–32.
[8] S. Laufer, J. Bajorath, *J. Med. Chem.* **2014**, *57*, 2167–2168.
[9] J. Bain, L. Plater, M. Elliott, N. Shpiro, C. J. Hastie, H. McLauchlan, I. Klevernic, J. S. C. Arthur, D. R. Alessi, P. Cohen, *Biochem. J.* **2007**, *408*, 297–315.
[10] L. A. Smyth, I. Collins, *J. Chem. Biol.* **2009**, *2*, 131–151.
[11] D. M. Goldstein, N. S. Gray, P. P. Zarrinkar, *Nat. Rev. Drug Discovery* **2008**, *7*, 391–397.
[12] M. I. Davis, J. P. Hunt, S. Herrgard, P. Ciceri, L. M. Wodicka, G. Pallares, M. Hocker, D. K. Treiber, P. P. Zarrinkar, *Nat. Biotechnol.* **2011**, *29*, 1046–1051.
[13] M. S. Cohen, C. Zhang, K. M. Shokat, J. Taunton, *Science* **2005**, *308*, 1318–1321.
[14] Q. Liu, Y. Sabnis, Z. Zhao, T. Zhang, S. J. Buhrlage, L. H. Jones, N. S. Gray, *Chem. Biol.* **2013**, *20*, 146–159.
[15] Y. Liu, N. S. Gray, *Nat. Chem. Biol.* **2006**, *2*, 358–364.
[16] Z. A. Knight, K. M. Shokat, *Cell* **2007**, *128*, 425–430.
[17] A. Zask, J. Murphy, G. A. Ellestad, *Chirality* **2013**, *25*, 265–274.
[18] H. Takahashi, S. Wakamatsu, H. Tabata, T. Oshitari, A. Harada, K. Inoue, H. Natsugari, *Org. Lett.* **2011**, *13*, 760–763.
[19] Y. Nakama, O. Yoshida, M. Yoda, K. Araki, Y. Sawada, J. Nakamura, S. Xu, K. Miura, H. Maki, H. Arimoto, *J. Med. Chem.* **2010**, *53*, 2528–2533.
[20] S. R. LaPlante et al., *J. Med. Chem.* **2014**, *57*, 1944–1951.
[21] J. Clayden, W. J. Moran, P. J. Edwards, S. R. LaPlante, *Angew. Chem. Int. Ed.* **2009**, *48*, 6398–6401; *Angew. Chem.* **2009**, *121*, 6516–6520.
[22] S. R. LaPlante, P. J. Edwards, L. D. Fader, A. Jakalian, O. Hucke, *ChemMedChem* **2011**, *6*, 505–513.
[23] S. R. LaPlante, L. D. Fader, K. R. Fandrick, D. R. Fandrick, O. Hucke, R. Kemper, S. P. F. Miller, P. J. Edwards, *J. Med. Chem.* **2011**, *54*, 7005–7022.
[24] J. Porter et al., *Bioorg. Med. Chem. Lett.* **2009**, *19*, 1767–1772.
[25] L. Xing et al., *ChemMedChem* **2012**, *7*, 273–280.
[26] S. R. Laplante et al., *J. Med. Chem.* **2014**, *57*, 1944–1951.
[27] K. Yoshida, R. Itoyama, M. Yamahira, J. Tanaka, O. Lozach, E. Durieu, T. Fukuda, F. Ishibashi, L. Meijer, M. Iwao, *J. Med. Chem.* **2013**, *56*, 7289–7301.
[28] Y. Liu, A. Bishop, L. Witucki, B. Kraybill, E. Shimizu, J. Tsien, J. Ubersax, J. Blethrow, D. O. Morgan, K. M. Shokat, *Chem. Biol.* **1999**, *6*, 671–678.
[29] L. Tatton, G. M. Morley, R. Chopra, A. Khwaja, *J. Biol. Chem.* **2003**, *278*, 4847–4853.
[30] L. Widler, J. Green, M. Missbach, M. Susa, E. Altman, *Bioorg. Med. Chem. Lett.* **2001**, *11*, 849–852.
[31] S. M. Maddox, C. J. Nalbandian, D. E. Smith, J. L. Gustafson, *Org. Lett.* **2015**, *17*, 1042–1045.
[32] K. T. Barrett, A. J. Metrano, P. R. Rablen, S. J. Miller, *Nature* **2014**, *509*, 71–75.
[33] G. Bringmann, A. J. P. Mortimer, P. A. Keller, M. J. Gresser, J. Garner, B. Matthias, *Angew. Chem. Int. Ed.* **2005**, *44*, 5384–5427; *Angew. Chem.* **2005**, *117*, 5518–5563.
[34] L. L. Carr, D. A. Mankoff, B. H. Goulart, K. D. Eaton, P. T. Capell, E. M. Kell, J. E. Bauman, R. G. Martins, *Clin. Cancer Res.* **2010**, *16*, 5260–5268.
[35] S. A. Wells, J. E. Gosnell, R. F. Gagel, J. Moley, D. Pfister, J. A. Sosa, M. Skinner, A. Krebs, J. Vasselli, M. Schlumberger, *J. Clin. Oncol.* **2010**, *28*, 767–772.
[36] L. M. Mulligan, *Nat. Rev. Cancer* **2014**, *14*, 173–186.
[37] T. Barf, A. Kaptein, *J. Med. Chem.* **2012**, *55*, 6243–6262.
[38] X. Zhang, J. Gureasko, K. Shen, P. A. Cole, J. Kuriyan, *Cell* **2006**, *125*, 1137–1149.
[39] CCDC 1404370 contains the supplementary crystallographic data for this paper. These data are provided free of charge by The Cambridge Crystallographic Data Centre.

[40] We thank a reviewer for suggesting that the loss of potency of the atropisomeric analogues may be due to the optimal dihedral angle of ligand binding being significantly perturbed from the 90° that one would expect an atropisomer to ideally adopt. While we cannot preclude this possibility, we have performed DFT calculations (RB3LYP/6-31G(d) level of theory) to predict the energy profile of rotation around the axis in **2e** at 10° increments (see the Supporting Information). This analysis suggests that the rotational energy landscape is fairly flat (± 2 kcal mol^{-1}) for almost 90°, including the predicted dihedral angles of **2e** and **5**. Nonetheless, other atropisomers with larger substituents are likely to have narrower profiles, and such analyses will be crucial for target selection and design.